Autonomous Robots, Drones and Repeaters for Fast, Reliable, Low-Cost RFID Inventorying & Localization

Antonis Dimitriou
School of ECE, AUTH
Thessaloniki, Greece
antodimi@ece.auth.gr

Anastasios Tzitzis
School of ECE, AUTH
Thessaloniki, Greece
atzitzis@ece.auth.gr

Alexandros Filotheou
School of ECE, AUTH
Thessaloniki, Greece
alefilot@ece.auth.gr

Spyros Megalou
School of ECE, AUTH
Thessaloniki, Greece
smegalou@ece.auth.gr

Stavroula Siachalou
School of ECE, AUTH
Thessaloniki, Greece
ssiachal@ece.auth.gr

Aristidis R. Chatzistefanou
School of ECE, AUTH
Thessaloniki, Greece
raptopak@ece.auth.gr

Andreana Malama
School of ECE, AUTH
Thessaloniki, Greece
andmalama@gmail.com

Emmanouil Tsardoulias
School of ECE, AUTH
Thessaloniki, Greece
etsardou@ece.auth.gr

Konstantinos Panayiotou
School of ECE, AUTH
Thessaloniki, Greece
klpanagi@ece.auth.gr

Evaggelos Giannelos
School of ECE, TUC
Chania, Greece
egiannelos@isc.tuc.gr

Thodoris Vasiliadis
Trinity Systems
Thessaloniki, Greece
tvasilia@trinitysystems.gr

Ioannis Mouroutsos
Trinity Systems
Thessaloniki, Greece
mourouts@trinitysystems.gr

Ioannis Karanikas
Trinity Systems
Thessaloniki, Greece
jkaranikas@trinitysystems.gr

Loukas Petrou
School of ECE, AUTH
Thessaloniki, Greece
loukas@eng.auth.gr

Andreas Symeonidis
School of ECE, AUTH
Thessaloniki, Greece
asymeon@eng.auth.gr

John Sahalos
AUTH, Greece &
UNIC, Cyprus
sahalos@auth.gr

Traianos Yioultsis
School of ECE, AUTH
Thessaloniki, Greece
traianos@ece.auth.gr

Aggelos Bletsas
School of ECE, TUC
Chania, Greece
aggelos@telecom.tuc.gr

Abstract—**This paper presents our latest results of our prototype robots and drones, aiming continuous inventorying and accurate real-time 3D localization of RFID tagged items. We have designed and constructed two ground robots, capable of autonomous inventorying in unknown regions, exploiting state-of-the-art methods from the field of robotics and RF-localization. Furthermore, we present our prototype drone, also capable of 3D inventorying and localization. In addition, we demonstrate the performance of our prototype RFID repeater, which also boosts the read-range of traditional RFID technology. The results of measurements campaigns conducted in different environments for the above prototypes are presented herein.**

Index Terms—**RFID, Inventorying, Robotics, Localization, Internet of Things**

I. Introduction

This work summarizes our latest findings in the context of the project Relief [1], where we aim to ensure autonomous 24/7 inventorying. The team has designed and built the following prototypes:

- Two ground robots. The robots are capable to create a 3D map of the surrounding environment [9]- [10]. They can perform Simultaneous Localization (of their own

pose) and Mapping (SLAM). They can safely navigate autonomously inside the map. They can dynamically create optimal paths, adjusting their decisions in real-time, depending on the changes of the surrounding environment. They avoid obstacles. Furthermore, the robots can interrogate all surrounding UHF RFID tags, and 3D localize them at cm accuracy in real time, thanks to the developed sophisticated algorithms [11]- [19].

- A drone. The drone is able to fly autonomously in exterior (GPS-enabled) areas, carrying out any pre-programmed mission-flight. The drone may also fly indoor in a semi-autonomous manner, avoiding collisions with the surrounding obstacles. The drone is also capable of 3D inventorying and localization of RFID tagged products [21]- [22].

- A UHF-RFID low-cost repeater. The repeater increases the reader-to-tag incident field, thus greatly increasing the read-range of the reader [25]- [26].

II. Ground Robots

In this section, we present the achieved performance by our two terrestrial inventorying and real-time localization robots, "Frida" and "Loci", shown in Figs.

A. Hardware

The two ground mobile robots are equipped with the ROBOTNIK RB-1 mobile base, and the Turtlebot mobile base, respectively. The former is heavier and may accommodate greater mass loads, and superstructures larger in height than the latter. Both robots are equipped with one 2D LIght Detection And Ranging (LIDAR) sensor, through which the robots may create a 2D map of the environment in which they are situated, and also localise themselves autonomously. For the purpose of creating a 3D map of their environment, the Turtlebot robot is equipped with one frontal RGBD image sensor, while the RB-1 robot is equipped with one frontal and two lateral RGBD sensors. The Turtlebot was equipped with one RFID reader, and four (two-by-two) laterally mounted lightweight antennas, at a maximum height of 1.5 m from the ground. In contrast, the RB-1 robot was equipped with two RFID readers, and eight (four-by-two) laterally mounted antennas, at a maximum height of 2.0 m. Both robots are equipped with small form factor on-board computers for the concentration of measurements by the various sensors, their on-line processing, robot self-localisation, robot autonomous motion commanding, and on-line RFID inventorying and 3D real-time localisation of tagged items.

B. Capabilities of the Ground Robots

In order for a mobile robot to perform autonomous RFID inventorying, we identify five algorithmic components: (i) a mapping algorithm, (ii) a robot-localisation algorithm, (iii) a path-planning algorithm, (iv) a motion controller, and (v) a RFID-localisation algorithm. The first solves one aspect of the SLAM problem (map-creation) in two [2] or three [3] dimensions. Both rest on the continuous integration and matching of successive LIDAR or RGBD measurements, usually considering an estimate of the robot's motion between two measurements, which is extracted via odometry. The existence of a map is a prerequisite for robot localisation, which refers to tracking the robot's pose (x, y, θ) over time and through space as the robot moves on the 2D ground plane. Robot localisation with the use of a LIDAR sensor is usually performed by employing a Kalman [5] or a Particle filter [6] [7]. It rests on the alignment of LIDAR measurements to the map of the environment in which the robot moves by considering the robot's motion model. In the case of RELIEF, both ground robots are of the unicycle model [8]. Once the map and the robot's pose are available, autonomous RFID inventorying refers to the robot's ability to traverse the map's (and therefore the environment's) free space without human input of motion commands. In order for a robot to move from its current pose estimate to a target pose in the environment's map, first a path-planning algorithm computes a path in the map that connects the two, under the constraint that the robot's footprint must avoid obstacles marked as such in the map. Popular approaches include the A* and Voronoi decomposition algorithms. If such a path exists, then it is inputted to the motion controller, which, considering the continuously-updated output of pose-tracking, and measurements from the LIDAR sensor actually inputs motion commands to the robot's wheels so that the path is followed. In our realisation of the controller, it was configured such that dynamic obstacles, meaning obstacles that reside only within the environment and not its map (such as persons or mobile machinery within the inventorying environment) were avoided on-the-fly by considering measurements from both the LIDAR and RGBD sensors. This capability removes the constraint of having to disrupt day-to-day operations when, for instance, people work within a warehouse in which the inventorying is performed, and supports continuous inventorying. Given the map's environment, and the capabilities of self-localisation and autonomous pose-to-pose navigation, vantage target poses may be concatenated in a cyclical manner so that the robot continuously and cyclically navigates to the vicinity of the RFID tags to be inventoried.

In our specific implementation, mapping is performed via the "karto" SLAM algorithm [4], robot-localisation through a modified version of the "amcl" algorithm [10], autonomous navigation via the "navfn" path-planner, and the "teb" motion controller [9], within the ROS suite.

C. Real Time 3D Localisation

The component accommodated on top of all robotics systems is the RFID-localisation algorithm. RFID localisation refers to the robot's ability to pinpoint the tagged objects into the created map of the environment. It rests on the integration of the tag's readings (acquired by the reader's antennas) and the antennas' locations (made available by the robot-localisation algorithm), such that a multi-antenna synthetic aperture (SAR) is generated. In the context of RELIEF, a novel SAR-based localization method has been developed, called Phase ReLock. According to it, the raw phase measurements collected along the multi-antenna aperture are initially unwrapped and in combination with a phase-distance model, they represent the input to a data-fit problem, where the model's coefficients account for the tag's unknown coordinates. The problem is solved in a least-square sense, while its convex-type property allows nonlinear optimization to converge rapidly to the problem's unique minimum. In contrast to other SAR-based methods, which employ exhaustive search over a grid [12] or particle swarm optimization [13], this effect supports the real-time application of Phase ReLock, providing online localisation of the tags as the robot navigates to the vicinity of them, while the estimations are continuously updated and improved as the collection of measurements is enriched with new samples. The proposed RFID localisation system is enhanced by the implementation of online performance evaluation. Tag estimations are accompanied by their confidence, quantified by the variance of their estimated coordinates. By evaluating such confidence metric, poor estimations based among others on inadequate measurements can be identified and treated accordingly.

The method has been explicitly presented for 2D localisation by a single antenna in [14]- [15], then was extended in 3D with a single antenna in [16]- [17] and is generalized in 3D space for multiple antennas in [18]. In this paper, a

new strategy is presented, according to which, a different version of Phase ReLock is dynamically applied, depending on the availability of measurements from the antennas located on the robots. In general, processing measurements collected by a minimum of two antennas is a prerequisite for localization in three dimensions. When this requirement is met, Phase ReLock 3D [18] is employed to construct a multi-antenna optimization problem and output the location of the tag in 3D space, accompanied by the corresponding confidence metric. Poor confidence mainly indicates that although the processed phase samples originated from at least two antennas, the amount of them was inadequate to achieve accurate 3D localisation. The estimation should be rejected and two-dimensional localisation is performed considering only the antenna-aperture that contributed the most samples; in case only a single antenna collected data, 2D localization is performed. Phase ReLock 2D [15] is applied to solve a single-antenna optimization problem and reconstruct the tag's location assuming that its height coincides with the antenna's. Poor confidence reflects an insufficient data contribution of the antenna and the estimated location is again discarded. Eventually, a rough estimation is made based on the minor available samples. According to it, tag's position is released perpendicular opposite to the antenna location at which, the maximum signal power was recorded.

As for inventorying speed, each robot has been constrained to move by as much as 25 cm/sec, and drop its velocity to as much as 5 cm/sec, dynamically adjusting its speed, depending on the tags' population.

D. Measurements

An excessive experimental campaign took place inside the school's library, where approximately 450 books were tagged with the Alien squiggle RFID tag, attached to the Higgs-4 IC. We have arranged the tags in different regions of the library, creating highly populated regions (300 tags were placed in a volume less than 40cm×60cm×160cm), regions with poor expected coverage performance (a series of tags were placed at 5cm from the ground - bottom shelf, where only the lowest antenna of the robot ensured partial coverage) and finally regions with sparse-tag-arrangement (25 tags within 60cm), in order to test the accuracy and the robustness of our system, under different situations. Thanks to the RGBD cameras, "Frida" created the 3D map shown in Fig. 1. Notice the fine-details captured by the robot, thanks to the RGBD cameras, placed at greater heights, thus successfully capturing the entire scene. A screenshot from one of the measurements inside the library is shown in Fig. 2, where the 3D localized tags are shown and updated in real-time in the bottom right corner within the map created by the robot. The entire video can be watched in [20].

Fig. 3 represents the tag configurations and compares the estimated and actual locations by pinpointing them inside the library's 2D map, while Fig. 4 summarizes the system's performance according to the adopted confidence-based strategy. 45% of the tag population was sufficiently read by at least
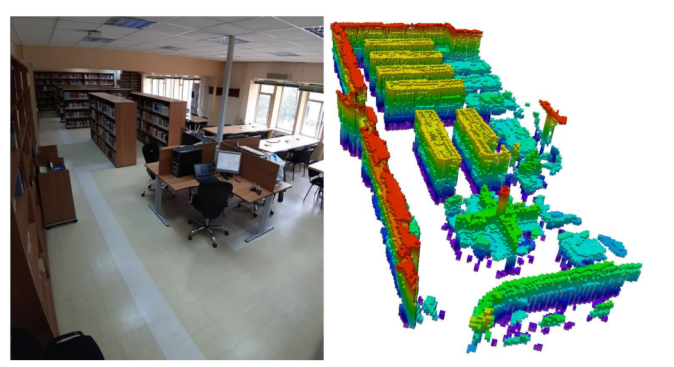

Fig. 1. Photo of the library and the corresponding 3D map, created by the robot.

Fig. 2. Photo of "Loci" in the School's library. "Frida" is shown in the bottom-left corner.

two antennas and ensured reliable 3D localization by [18], delivering a mean error or 18cm. 31% of the tags delivered adequate samples by a single antenna and therefore [15] was applied to perform 2D localization, reporting a mean error of 20cm, while the remaining 24% was estimated roughly with less accuracy due to inadequacy of measured samples. The algorithm achieved to locate approximately 450 tags within 20s (i.e. 45ms per tag), much faster than the data-collection time, verifying experimentally the real-time capability of the proposed system.

III. DRONE

A. Hardware

The aerial vehicle used in project RELIEF is an ItalDron EVO 4HSE, as shown in Fig. 5. It is equipped with four rotors, a high-capacity battery which yields a flight time of approximately 20 mins, a frontal analog FPV video sensor, an altitude meter, a GPS receiver, and most importantly for autonomous navigation, an autopilot board. The latter is connected via RF telemetry to a Ground Control Station (GCS), which may remotely control all aspects of vehicle flight, and to a remote controller (RC). In addition to these factory components, the vehicle was equipped with a distance sensor of 8 rays over a panoramic horizontal field of view, a 3D printed case for
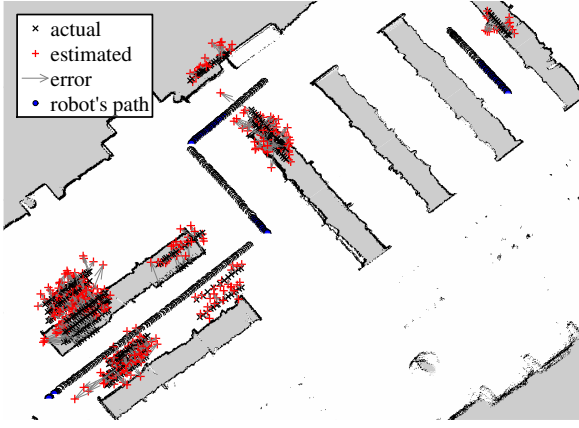
Fig. 3. Estimated and actual locations of tags pinpointed in the environment's 2D map.
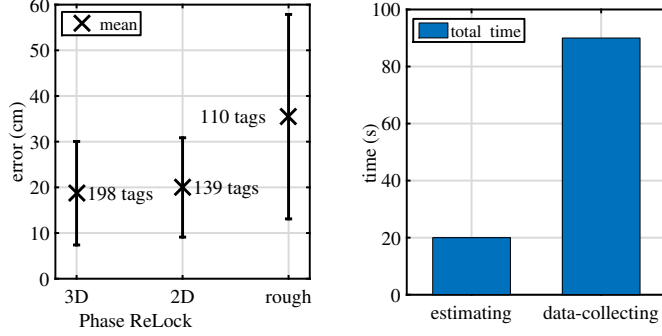

Fig. 4. Localization error and execution time of the proposed RFID-system.

housing the RFID reader, antenna, and wireless relay module. The distance sensor is used for navigation purposes in indoor circumstances, as its connection to the autopilot informs the latter in deciding whether manual (RC) maneuvers may result in collisions with obstacles, which are subsequently denied execution, therefore securing obstacle avoidance and denial of collision.

Fig. 5. Photo of the RFID-equipped drone.

B. Capabilities

The navigational operation of the aerial vehicle is distinct per—and depends on—the type of flight environment. In indoor environments, GPS reception is denied, and therefore so is autonomous navigation. RFID-inventorying is performed by navigating the vehicle manually via the RC to the vicinity of RFID tags, by selecting flight modes appropriate to the spatial configuration of the tags. We are flying the drone in "Altitude Hold" mode, where the downward-facing laser sensor secures flight at a specific height above the RFID-tracked equipment. In contrast, in outdoor environment, GPS reception enables autonomous flight. Modern mission planners and controllers (e.g. Mission Planner) enable autonomous take-off, navigation via waypoints, and landing at dm accuracy. A screenshot of the measurements, along with the environment of mission planner (real-time location of the drone) are shown in Fig. 6. The entire video of the measurements can be watched in [24], while the 3D map created by the camera is shown in Fig. 7.

Fig. 6. Drone and "mission planner" during measurements.

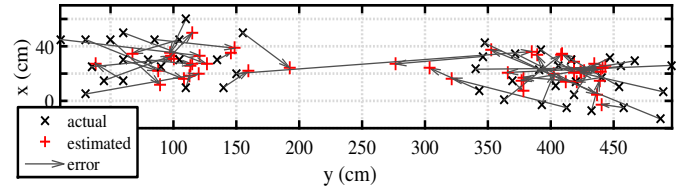
Fig. 7. 3D map of the area, created by the camera.

Fig. 8. Localization error, deploying fingerprinting technique, based on power.

C. Fingerprinting Localization

In order to keep the drone as lightweight as possible, we haven't installed the required sensory equipment that would allow the drone to accurately estimate each own pose, as was the case in the terrestrial robots. Consequently, we have deployed the fingerprinting algorithms, presented in [21]- [22], based on "Landmarc" [23]. According to these methods, 3D localization of target tags is accomplished in real time by

comparing their power and phase measurements with the corresponding measurements collected from reference tags, i.e. tags placed at known locations, in neighboring time-instances.

D. Measurements

We have attached approximately 100 passive UHF RFID tags at known positions on top of two millimeter papers, over an area of 100cm × 500cm, which represents the search space. the reference tags were placed at 25cm to 50cm intervals, but there is a gap of 2m between the two millimeter papers with no reference tags, which greatly deteriorates the accuracy of localization. The drone flew above this region three times as shown in the measurements' video, publicly available in [24]. During the flight, the measured RFID data were sent to the ground station, which performed real-time localization. The corresponding results from the first section of measurements are shown in Fig. 8. We have achieved a mean error of 53,87cm and a standard deviation of 37.8cm, which is acceptable for most inventorying applications.

IV. REPEATER

In this section, we present our prototype UHF forward-link repeater [25]- [26] and its performance.

A. Hardware

The prototype UHF-RFID repeater consists of the following elements: i) a directional antenna (antenna 1 in Fig. 9), facing the reader antenna, ii) a band-pass filter iii) an RF power limiter, iv) a low noise amplifier and v) a directional antenna (antenna 2 in Fig. 9), facing the tag. The incident signal from the reader is received by antenna 1, filtered by the filter, limited if the incident RF power is above a given threshold, amplified by the amplifier and re-emitted by antenna 2.
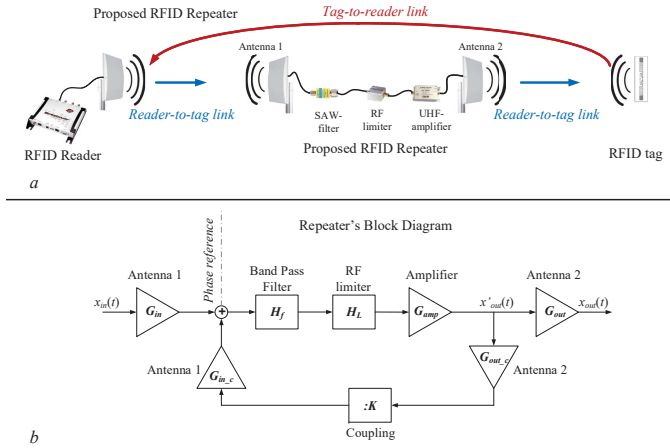

Fig. 9. Representation of the prototype repeater.

B. Capabilities

The repeater is designed with circularly polarized microstrip antennas with inverse polarization handedness offering a decoupling of more than 65dB in the entire European operation band of UHF-RFID systems. The proposed structure *i)*maintains a small volume, despite the strict decoupling limitation *ii)* maximises the gain by fully utilising the circularly polarized incident field from the reader antenna and *iii)* improves the interrogation accuracy of RFID tags. In addition, multiple repeaters can be used in a waterfall connection providing enough power to a tag at any distance.

Furthermore, the repeater can be placed on top of low-cost autonomous robots taking advantage of their mobility, further improving the interrogation range and accuracy. The motion of the robot results to multipath changes, leading to identification of passive RFID tags even at Non-Line-Of-Sight (NLOS) locations.

C. Measurements

The prototype structure was measured in two cases. In the first case, range measurements with a static repeater took place outdoors. The repeater was placed in various distances and the interrogation range was measured as shown in Fig. 10. By placing the repeater at a distance of 55m from the reader, interrogation of passive RFID tags was achieved at a range of 59m (see video at [27]).
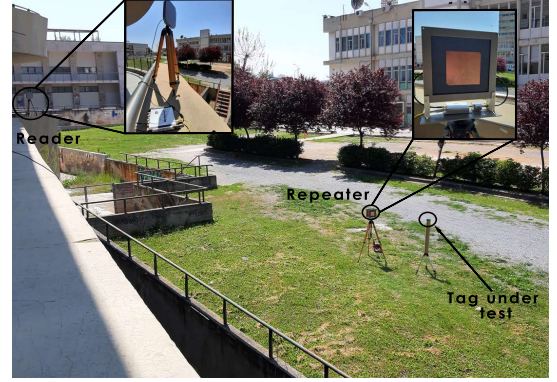

Fig. 10. View from reader and from tag for 60m-long successful passive RFID-tag identification.

In the second case, the repeater was placed on top of an autonomous robot. Measurements took place in a rectangular room, including 5 rows of desks with computers as shown in Fig. 11. 48 passive RFID tags were attached to four "banners", 15 meters away from the reader antenna. The mobile repeater starts its journey from point A and reaches the end point B after passing successively through each corridor. By changing the position of the repeater over time, the tags are illuminated from different angles, while the robot is also involved in shaping the fading pattern. As the robot moves along paths closest to the tag, the number of recognized tags increases until it reaches an astonishing 46/48 successfully recognized tags, including 10 tags under NLOS conditions (see video at [28]).

V. CONCLUSIONS

In this paper, we have presented our latest results from the project "Relief" [1]. We have developed two ground robots, capable to perform autonomously perform inventorying and
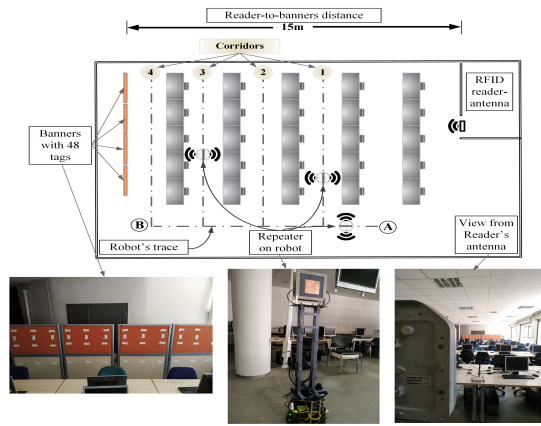
Fig. 11. Measurements' setup of repeater on top of robot

real-time accurate 3D localization of RFID tags with cm accuracy. Our robots achieve 3D accuracy with mean error in the order of 20cm, while the results are depicted on the map created by the robot, during the inventorying process. We have presented our latest measurements from the drone, where fingerpinting localization accomplished a mean error in the order of 50cm. Finally, our prototype repeater can be deployed either in fixed installation, ensuring order of magnitude increase in the read-range or on top of the robot, allowing interrogation of "hidden" tags from a far-way fixed reader.

REFERENCES

[1] Relief. Intelligent Repeaters and Robots for Fast, Reliable, Low-Cost RFID Inventorying & Localization. Accessed May. 13, 2021 [Online]. Available:https://relief.web.auth.gr/language/en/home/.

[2] G. Grisettiyz, C. Stachniss and W. Burgard, "Improving Grid-based SLAM with Rao-Blackwellized Particle Filters by Adaptive Proposals and Selective Resampling," Proceedings of the 2005 IEEE International Conference on Robotics and Automation, pp. 2432-2437, 2005, doi: 10.1109/ROBOT.2005.1570477.

[3] M. Labbé and F. Michaud, "RTAB-Map as an open-source lidar and visual simultaneous localization and mapping library for large-scale and long-term online operation," J Field Robotics, vol. 35, pp. 416– 446, 2019, doi: 10.1002/rob.21831.

[4] K. Konolige, G. Grisetti, R. Kümmerle, W. Burgard, B. Limketkai and R. Vincent, "Efficient Sparse Pose Adjustment for 2D mapping," 2010 IEEE/RSJ International Conference on Intelligent Robots and Systems, pp. 22-29, 2010, doi: 10.1109/IROS.2010.5649043.

[5] P. Maybeck, Stochastic Models, Estimation and Control, Volume 1, Academic Press, New York, 1979.

[6] F. Dellaert, D. Fox, W. Burgard and S. Thrun, "Monte Carlo localization for mobile robots," Proceedings 1999 IEEE International Conference on Robotics and Automation (Cat. No.99CH36288C), Detroit, MI, USA, 1999, pp. 1322-1328 Volume 2, doi: 10.1109/ROBOT.1999.772544.

[7] D. Fox, "Adapting the Sample Size in Particle Filters Through KLD-Sampling," Int J Rob Res , vol. 22(12), pp. 985–1003, 2003, doi: 10.1177/0278364903022012001.

[8] F. Kappeler, "Unicycle Robot", 2007. Accessed: 24 May 2021 [Online]. Available: https://www.epfl.ch/labs/la/wp-content/uploads/2018/08/Kappeler.Rapport.pdf.pdf

[9] A. Filotheou, E. G. Tsardoulias, A. Dimitriou, A. L. Symeonidis and L. Petrou, "Quantitative and qualitative evaluation of ROS-enabled local and global planners in 2D static environments", J. Intell. Robot. Syst., vol. 98, pp. 567-601, 2020.

[10] A. Filotheou, E. G. Tsardoulias, A. G. Dimitriou, A. L. Symeonidis and L. Petrou, "Pose selection and feedback methods in tandem combinations of particle filters with scan-matching for 2D mobile robot localisation," J. Intell. Robot. Syst., vol. 100, pp. 925-944, 2020.

[11] A. G. Dimitriou, S. Siachalou, E. Tsardoulias, L. Petrou, "Robotics Meets RFID for Simultaneous Localization (of Robots and Objects) and Mapping (SLAM) – a Joined Problem," in Wireless Power Transmission for Sustainable Electronics: COST WiPE-IC1301, John Wiley and Sons, March 2020. Inc. https://doi.org/10.1002/9781119578598.ch7.

[12] A. Motroni et al., "SAR-Based Indoor Localization of UHF-RFID Tags via Mobile Robot," 2018 International Conference on Indoor Positioning and Indoor Navigation (IPIN), 2018, pp. 1-8, doi: 10.1109/IPIN.2018.8533847.

[13] F. Bernardini et al., "Particle Swarm Optimization in SAR-Based Method Enabling Real-Time 3D Positioning of UHF-RFID Tags," in IEEE Journal of Radio Frequency Identification, vol. 4, no. 4, pp. 300-313, Dec. 2020, doi: 10.1109/JRFID.2020.3005351.

[14] A. Tzitzis, S. Megalou, S. Siachalou, T. Yioultsis, A. Kehagias, E. Tsardoulias, A. Filotheou, A. Symeonidis, L. Petrou, A. G. Dimitriou, "Phase ReLock - Localization of RFID Tags by a Moving Robot," 2019 13th European Conference on Antennas and Propagation (EuCAP), 2019, pp. 1-5.

[15] A. Tzitzis et al., "Localization of RFID Tags by a Moving Robot, via Phase Unwrapping and Non-Linear Optimization," in IEEE Journal of Radio Frequency Identification, vol. 3, no. 4, pp. 216-226, Dec. 2019, doi: 10.1109/JRFID.2019.2936969.

[16] A. Tzitzis, S. Megalou, S. Siachalou, E. Tsardoulias, T. Yioultsis and A. G. Dimitriou, "3D Localization of RFID Tags with a Single Antenna by a Moving Robot and "Phase ReLock"," 2019 IEEE International Conference on RFID Technology and Applications (RFID-TA), Pisa, Italy, 2019, pp. 273-278, doi: 10.1109/RFID-TA.2019.8892256.

[17] A. Tzitzis et al., "Trajectory Planning of a Moving Robot Empowers 3D Localization of RFID Tags with a Single Antenna," in IEEE Journal of Radio Frequency Identification, doi: 10.1109/JRFID.2020.3000332.

[18] A. Tzitzis, A. C. Raptopoulos, T. Yioultsis and A. G. Dimitriou, "A Real-Time Multi-Antenna SAR-based method for 3D localization of RFID Tags by a Moving Robot," in IEEE Journal of Radio Frequency Identification, doi: 10.1109/JRFID.2021.3070409.

[19] A. Tzitzis et al., "Real-time 3D localization of RFID-tagged products by ground robots and drones with commercial off-the-shelf RFID equipment: Challenges and Solutions," 2020 IEEE International Conference on RFID (RFID), Orlando, FL, USA, 2020, pp. 1-8, doi: 10.1109/RFID49298.2020.9244904.

[20] Video demo of RFID Robot Inventorying - Relief Project. url: https://youtu.be/bo4lMI640DY. Accessed May. 13, 2021 [Online]. Available:https://youtu.be/bo4lMI640DY.

[21] S. Megalou, A. Tzitzis, S. Siachalou, T. Yioultsis, J. Sahalos, E. Tsardoulias, A. Filotheou, A. Symeonidis, L. Petrou, A. Bletsas, A. G. Dimitriou, "Fingerprinting Localization of RFID tags with Real-Time Performance-Assessment using a Moving Robot," 13th European Conference on Antennas and Propagation, Krakow, Poland, March 2019.

[22] S. Siachalou, S. Megalou, A. Tzitzis, E. Tsardoulias, A. Bletsas, J. Sahalos, T. Yioultsis, A. G. Dimitriou, "Robotic Inventorying and Localization of RFID Tags, Exploiting Phase-Fingerprinting," 2019 IEEE International Conference on RFID-Technology and Applications, RFID-TA 2019, Pisa, Italy, September 2019.

[23] L. M. Ni, and Y. Liu, "LANDMARC: Indoor Location Sensing Using Active RFID," Wireless Networks, vol. 10, no. 6, pp. 701–710, 2004.

[24] Video demo of RFID Drone Inventorying - Relief Project. Accessed May. 13, 2021 [Online]. Available: https://youtu.be/0YFQzpWgEd4.

[25] A. G. Dimitriou, "Design, Analysis, and Performance Evaluation of a UHF RFID Forward-Link Repeater," in IEEE Journal of Radio Frequency Identification, vol. 4, no. 2, pp. 73-82, June 2020, doi: 10.1109/JRFID.2019.2953785.

[26] S. Megalou, A. G. Dimitriou, A. Tzitzis and T. V. Yioultsis, "Design and Fabrication of a Compact, Low-Cost UHF-RFID Repeater, Exploiting Circular Cross-Polarization," in IEEE Journal of Radio Frequency Identification, vol. 5, no. 1, pp. 64-74, March 2021, doi: 10.1109/JRFID.2020.3040439.

[27] Video demo of a tag being read at 60m thanks to the repeater - Relief Project. Accessed May. 13, 2021 [Online]. Available: https://youtu.be/9vvon7SLk84.

[28] Video demo of the repeater on top of the robot - Relief Project. Accessed May. 13, 2021 [Online]. Available: https://youtu.be/U7DZJKOYX7g.